Equatorial Pacific tropical instability vortices in October 1994

PS44A 2270

L. R. Benjamin, P. Flament - Department of Oceanography, University of Hawaii at Manoa

1. Introduction

In the equatorial Pacific:

1. Mostly zonal winds drive mostly zonal currents.
2. Poleward Ekman transport leads to equatorial upwelling.
3. North Equatorial Front (NEF) forms at north edge of upwelled waters and develops perturbations.
4. There are 2 kinds of instabilities: ELW and TIV.
5. Equatorial long waves (ELW) form at equator and propagate quickly westward (~0.8 m/s).
6. Tropical instability vortices (TIV) are cyclonic vortices with 500-km diameter that form at northward cold intrusions in the NEF and propagate more slowly westward (~0.4 m/s).

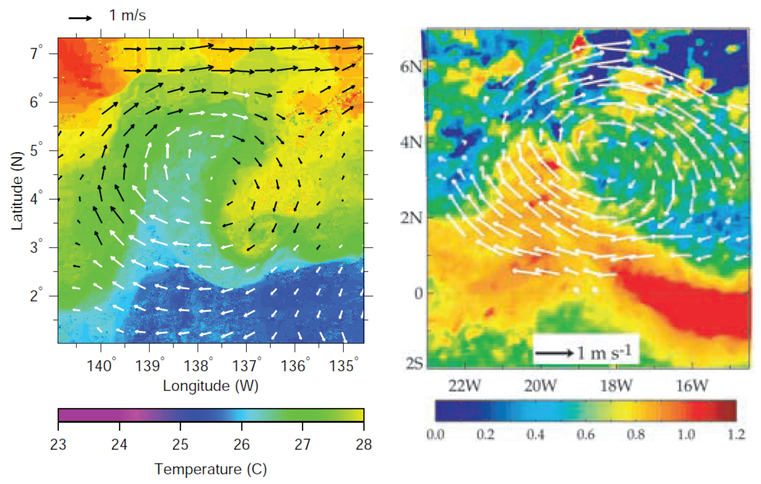

Figure 1. Sea surface temperature (color) and velocity structure (arrows) of TIV from (left) Flament et al. [1996] and (right) Menkes et al. [2002].

2. Methodology

Because of moving nature of TIVs, data from the following sources was shifted into a frame of reference moving zonally at -0.4 m/s with the plots made at 1200 UTC on 03/10/1994 (see Flament et al., 1996; Kennan and Flament, 2000; and Menkes et al., 2002):

1. Sea surface temperature: Pathfinder 4-km satellite temperatures
2. Sea surface height: Topex-Poseidon satellite altimetry
3. Vertically-polarized (VV) L-band synthetic aperture radar from SIR-C

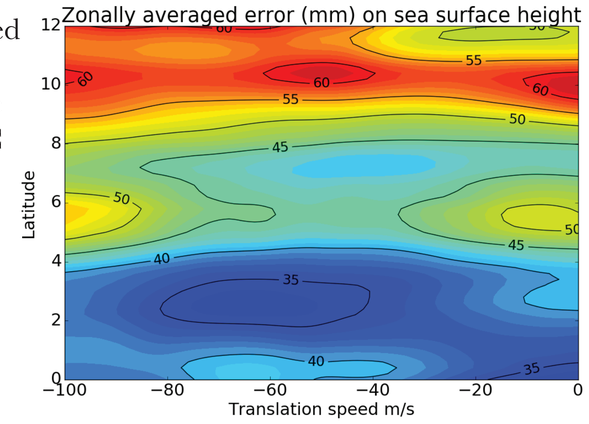

Figure 2. Zonally-averaged errors in sea surface height (mm) with translation speed. The translation speed is the speed at which the frame of reference moves. TIV are found at 2 to 8 N, so translation speeds of 0.3 to 0.5 m/s, errors are minimized.

3. Results

Buoy temperatures show record of TIV passage: Temperature at 140 m at 5 N, 140 W (cyan line in Figure 3) is in the thermocline, and it reflects the influence of increased pressure at the surface on the thermocline depth. High surface pressure at the surface can be an indication of a passing TIV (middle panel in Figure 5), so the higher temperatures at 140 m on days 255 to 270 were likely due to the passage of western TIV in Figure 5.

Two TIV with different sea level and velocity characteristics are present: There were two TIV present between 130 W and 150 W in Figure 5: the one centered at 6 N, 143 W has a stronger sea level effect, while the one centered at 4 N, 134 W has a sharper associated sea surface gradient as thus a stronger cyclogeostrophic velocity (top panel, Figure 5).

Sea surface temperature fronts align well with sea surface height domes associated with TIV: The sea surface temperatures in the bottom panel of Figure 5 show the trailing frontal edges approximately in the middle of the sea surface height domes in the middle panel.

Some fronts detected in synthetic aperture radar backscatter align well with sea surface temperature fronts: Fronts detected in synthetic aperture radar (e.g., Figure 4), which are the result of surface roughness changes (Figure 6) are drawn on the bottom panel of Figure 5 in black. The three fairly straight fronts in the western side slign well with the cold intrusion centered at 144 W, while the eastern curved front may be associated with the eastern cold intrusion.

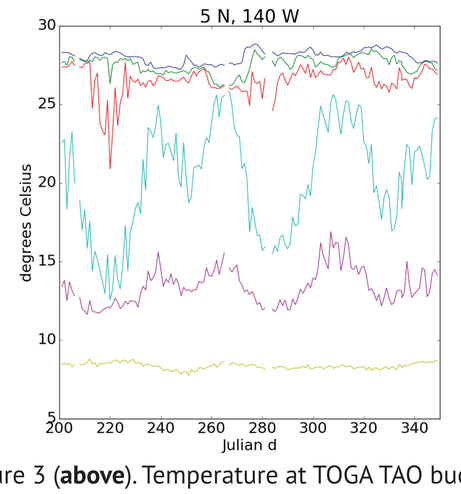

Figure 3 (**above**). Temperature at TOGA TAO buoy at 5 N, 140W at 1 m (blue), 80 m (green), 100 m (orange), 140 m (cyan), 180 m (violet), and 500 m (yellow).

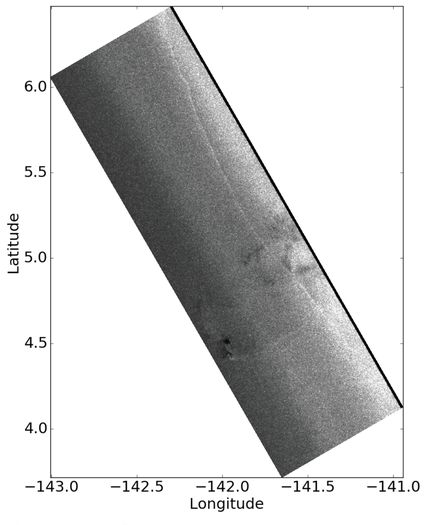

Figure 4 (**above**). Synthetic aperture radar backscatter on 07/10/1994, translated at 0.4 m/s eastward to project its location on 03/10/1994. This is the westernmost front in the bottom panel of Figure 5.

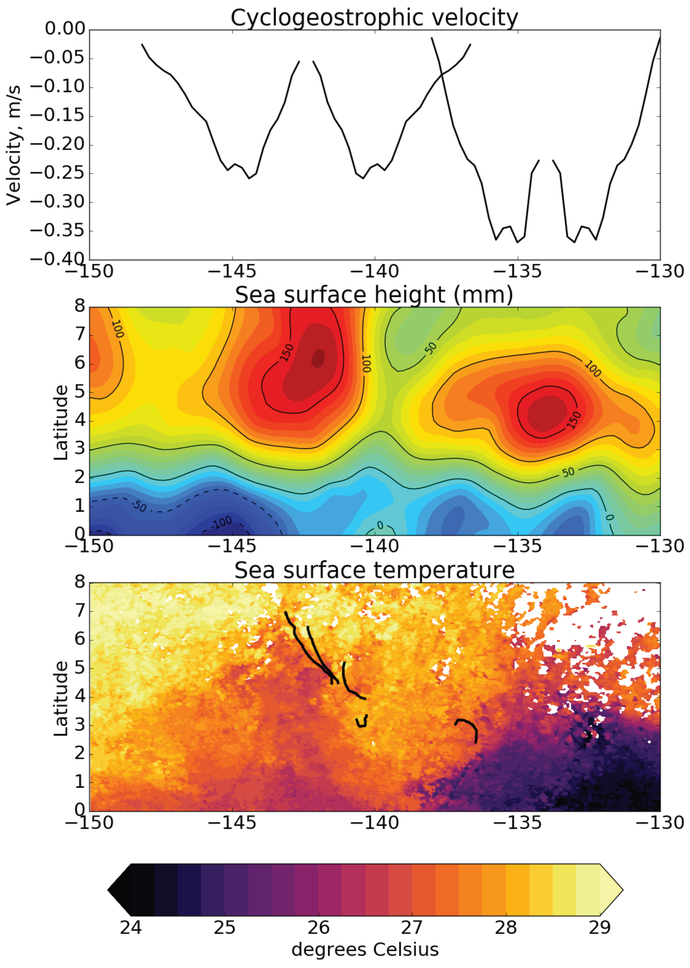

Figure 5 (**above**). Top: Cyclogeostrophic velocity calculated from Topex-Poseidon sea surface height. Middle: Sea surface height in mm over the region 130 to 150 W. Bottom: Sea surface temperature with 5 fronts determined by synthetic aperture radar backscatter overlain in black.

Figure 6 (**below**). Photograph taken in August 1994 of enhanced whitecapping at North Equatorial Front. Changes in surface roughness produce fronts visible in synthetic aperture radar (Figure 4).

Next steps

1. Examine high-resolution C-, L-, and X-band synthetic aperture radar images for further fronts
2. Examine directional spectra of above images for refraction of wave fronts
3. Determine if refraction is evidence of rotational currents of TIV

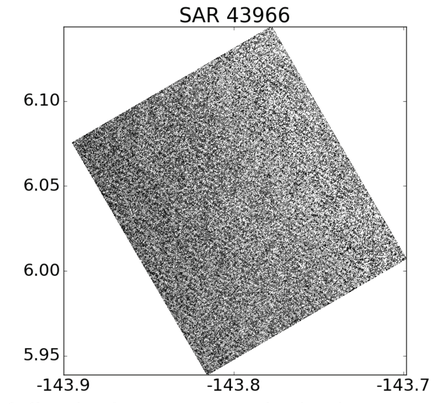

Figure 6. Synthetic aperture radar backscatter on 07/10/1994, with spatial resolution of 25 m. Dark and light bands are wave fronts with wavelength ~300 km. Strong currents can refract wave fronts, which can be detected with directional spectra.

References

Flament et al., 1996; Nature 383, 610 - 613.
Kennan and Flament, 2000; JPO 30, 2277 - 2301.
Menkes et al., 2002; GRL 29, 48.1 - 48.4.

Lindsey R. Benjamin
lrb@hawaii.edu
+1.808.956.7739
1000 Pope Road
Honolulu, HI 96822

SCHOOL OF OCEAN AND EARTH SCIENCE AND TECHNOLOGY
UNIVERSITY OF HAWAI'I AT MĀNOA